

Recombination dynamics of a 268 nm emission peak in $\text{Al}_{0.53}\text{In}_{0.11}\text{Ga}_{0.36}\text{N}/\text{Al}_{0.58}\text{In}_{0.02}\text{Ga}_{0.40}\text{N}$ multiple quantum wells

T. Onuma

Institute of Applied Physics and Graduate School of Pure and Applied Sciences, University of Tsukuba, 1-1-1 Tennodai, Tsukuba 305-8573, Japan and NICP, ERATO, Japan Science and Technology Agency, Kawaguchi 332-0012, Japan

S. Keller, S. P. DenBaars, J. S. Speck, S. Nakamura, and U. K. Mishra

Department of Electrical and Computer Engineering, University of California, Santa Barbara, California 93106, Department of Materials Engineering, University of California, Santa Barbara, California 93106, and NICP, ERATO, Japan Science and Technology Agency, Kawaguchi 332-0012, Japan

T. Sota

Department of Electrical Engineering and Bioscience, Waseda University, 3-4-1 Ohkubo, Shinjuku 169-8555, Japan

S. F. Chichibu^{a)}

Institute of Applied Physics and Graduate School of Pure and Applied Sciences, University of Tsukuba, 1-1-1 Tennodai, Tsukuba 305-8573, Japan and NICP, ERATO, Japan Science and Technology Agency, Kawaguchi 332-0012, Japan

(Received 26 August 2005; accepted 6 February 2006; published online 17 March 2006)

Recombination dynamics of the 268 nm photoluminescence (PL) peak in a quaternary $\text{Al}_{0.53}\text{In}_{0.11}\text{Ga}_{0.36}\text{N}/\text{Al}_{0.58}\text{In}_{0.02}\text{Ga}_{0.40}\text{N}$ multiple quantum well (MQW) grown on relaxed AlGaIn templates were studied. Although the polarization field in the compressively strained $\text{Al}_{0.53}\text{In}_{0.11}\text{Ga}_{0.36}\text{N}$ wells was as high as 1.6 MV/cm, the value of integrated PL intensity at 300 K divided by that at 8 K (η_{int}) was as high as 1.2%. The value was similar to that obtained for the 285 nm PL peak in an $\text{Al}_{0.30}\text{Ga}_{0.70}\text{N}/\text{Al}_{0.70}\text{Ga}_{0.30}\text{N}$ MQW (1.3%), though the AlN molar fraction in the wells was higher by a factor of 1.7. According to these results and the fact that time-resolved PL signal exhibited a *stretched exponential* decay shape, the improved η_{int} of the AlInGaIn wells was attributed to a beneficial effect of the exciton localization as is the case with InGaIn alloys; doping or alloying with InN was confirmed to work also on AlGaIn in improving η_{int} to realize deep UV optoelectronic devices. © 2006 American Institute of Physics. [DOI: 10.1063/1.2186109]

Wurzite $\text{Al}_x\text{In}_y\text{Ga}_{1-x-y}\text{N}$ quaternary alloys are a possible candidate for the realization of UV light emitters and detectors. Because deep UV emitters operating at a wavelength shorter than 280 nm have a variety of significant applications, a number of attempts¹⁻⁵ have been made to shorten the operating wavelength of GaN/AlGaIn (Ref. 1 and 2) or AlGaIn/AlGaIn (Ref. 3-5) quantum well (QW) light-emitting diodes (LEDs). As a result, LEDs with a wavelength as short as 250 nm have been demonstrated,⁴ although the external quantum efficiency is yet far lower than that of blue and green InGaIn-based LEDs.⁶

In order to improve the efficiency η of AlGaIn-based LEDs, three fundamental approaches have been made. One is to reduce the density of nonradiative recombination centers (NRCs) by reducing the threading dislocation (TD) density using lateral growth techniques^{1,7} or GaIn substrates.³ The second one is to reduce the magnitude of the internal electric field (F_{int}) in the QWs due to the spontaneous⁸ and piezoelectric^{9,10} polarization, because F_{int} reduces the electron-hole wavefunction overlapping through the quantum-confined Stark effects (QCSE). Indeed, reduced F_{int} has been demonstrated for $\text{Al}_{0.12}\text{In}_{0.04}\text{Ga}_{0.84}\text{N}/\text{Al}_{0.30}\text{In}_{0.01}\text{Ga}_{0.69}\text{N}$ quaternary multiple quantum wells (MQWs).¹¹ The third one is to dope or alloy with InN,^{5,12}

since the exciton localization¹⁰ into the In-related localizing centers¹³⁻¹⁵ greatly improves η in InGaIn alloys. However, the operation wavelength was limited to longer than 300 nm.

In this letter, results of CW photoluminescence (PL) and temperature-dependent time-resolved PL (TRPL) measurements on $\text{Al}_{0.53}\text{In}_{0.11}\text{Ga}_{0.36}\text{N}/\text{Al}_{0.58}\text{In}_{0.02}\text{Ga}_{0.40}\text{N}$ MQWs exhibiting emission peaks shorter than 280 nm are shown to analyze the effect of F_{int} and to confirm the beneficial effect of exciton localization in $\text{Al}_x\text{In}_y\text{Ga}_{1-x-y}\text{N}$ alloys. Value of the internal quantum efficiency (η_{int}), which is defined as the integrated PL intensity at particular temperature divided by that at 8 K, for the $\text{Al}_{0.53}\text{In}_{0.11}\text{Ga}_{0.36}\text{N}$ MQW was 1.2% at 300 K. The value was similar to that for a ternary $\text{Al}_{0.30}\text{Ga}_{0.70}\text{N}/\text{Al}_{0.70}\text{Ga}_{0.30}\text{N}$ MQW (1.3%), although the AlN molar fraction in the wells was higher by a factor of 1.7.

Lattice-relaxed $\text{Al}_{0.63}\text{Ga}_{0.37}\text{N}$ templates, of which TD density was approximately $3 \times 10^{10} \text{ cm}^{-2}$,¹⁶ were grown by low-pressure metalorganic vapor phase epitaxy on a (0001) Al_2O_3 substrate using a 14-nm-thick $\text{Al}_{0.63}\text{Ga}_{0.37}\text{N}$ low-temperature nucleation layer. Five-period 2.9- and 3.8-nm-thick $\text{Al}_x\text{In}_{0.11}\text{Ga}_{0.89-x}\text{N}$ ($x=0.53$ and 0.33)/7.3-nm-thick $\text{Al}_{0.58}\text{In}_{0.02}\text{Ga}_{0.40}\text{N}$ MQWs were grown on the Si-doped 1.24- μm -thick templates. For comparison, 20 period 2.0- to 7.6-nm-thick $\text{Al}_{0.30}\text{Ga}_{0.70}\text{N}/7$ -nm-thick $\text{Al}_{0.70}\text{Ga}_{0.30}\text{N}$ MQWs were grown on the undoped 1- μm -thick templates.¹⁶ Both MQWs were pseudomorphically grown on the templates, and nominal alloy composi-

^{a)} Author to whom correspondence should be addressed; electronic mail: optoelec@bk.tsukuba.ac.jp

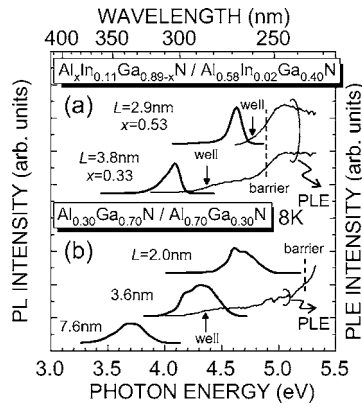


FIG. 1. PL and PLE spectra of (a) five period 2.9- and 3.8-nm-thick $\text{Al}_x\text{In}_{0.11}\text{Ga}_{0.89-x}\text{N}/7.3\text{-nm-thick Al}_{0.58}\text{In}_{0.02}\text{Ga}_{0.40}\text{N}$ and (b) 20 period 2.0- to 7.6-nm-thick $\text{Al}_{0.30}\text{Ga}_{0.70}\text{N}/7\text{-nm-thick Al}_{0.70}\text{Ga}_{0.30}\text{N}$ MQWs at 8 K. The arrows and broken lines indicate the energy positions of the effective band gap $E_{g,\text{eff}}$ of the well and barrier layers, respectively.

tions were estimated from the stained lattice parameters and growth parameters.

PL was excited by a frequency-tripled mode-locked (~ 100 fs) $\text{Al}_2\text{O}_3:\text{Ti}$ laser ($40\text{--}60$ nJ/cm²), of which wavelength was chosen between 242 and 260 nm to selectively excite the wells. The repetition rate was reduced from 80 MHz to the desired frequency using the acousto-optic modulator. Photoluminescence excitation (PLE) spectrum was recorded by monitoring the lower energy tail of the near-band edge PL at 8 K using a monochromatic light source.

Steady-state optical responses of the AlInGaN MQWs resembled those of InGaN.^{6,9,10,13,14,17} PL spectra of $\text{Al}_x\text{In}_{0.11}\text{Ga}_{0.89-x}\text{N}$ wells exhibited a peak at 4.627 eV (268 nm), of which the full width at half maximum (FWHM) was 116 meV, for $x=0.53$ and one at 4.086 eV (FWHM = 155 meV) for $x=0.33$ at 8 K, as shown in Fig. 1(a). The FWHM values were much smaller than those obtained for the AlGaIn wells being 265–380 meV, as shown in Fig. 1(b). PLE spectra of the AlInGaN wells exhibited the signals due to the wells and barriers. The effective band gap energy ($E_{g,\text{eff}}$) was defined as the energy at which the PLE intensity decreased to its half the maximum. $E_{g,\text{eff}}$ values were 4.770 eV for $x=0.53$, 4.374 eV for $x=0.33$, and 4.897 eV for the barriers, as shown by the arrows and vertical broken line in Fig. 1(a). Accordingly, the Stokes-type shifts were 143 meV for $x=0.53$ and 288 meV for $x=0.33$, implying the presence of band gap inhomogeneity exaggerated by QCSE.^{9,10} The low temperature PLE spectra of the $\text{Al}_{0.30}\text{Ga}_{0.70}\text{N}/\text{Al}_{0.70}\text{Ga}_{0.30}\text{N}$ MQWs exhibited similar broad absorption tail, and the PL peak shifted to the lower energy by 1 eV with increasing the well thickness L from 2.0 to 7.6 nm. Since the peak energy (3.7 eV) for $L=7.6$ nm was lower than $E_{g,\text{eff}}$ of strain-free $\text{Al}_{0.30}\text{Ga}_{0.70}\text{N}$ (4.064 eV),¹⁸ presence of QCSE in the compressively strained $\text{Al}_{0.30}\text{Ga}_{0.70}\text{N}$ wells is obvious. The magnitude of F_{int} is estimated to be 1.6 MV/cm using the linear approximation between the PL peak energy and L . As a consequence of the reduced oscillator strength, PL lifetime (τ_{PL}) at 10 K, which corresponds to the radiative lifetime, increased from 1.09–3.83 ns for $L < 3.6$ nm to 640–825 ns for $L \geq 6.5$ nm (data not shown). The magnitude of F_{int} in the compressively strained $\text{Al}_{0.53}\text{In}_{0.11}\text{Ga}_{0.36}\text{N}$ wells might be the same order,

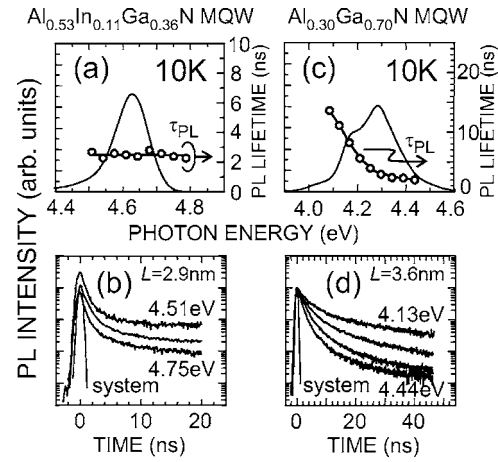


FIG. 2. (a) PL spectrum and energy-resolved τ_{PL} values and (b) corresponding TRPL signals measured at 10 K for the 2.9-nm-thick $\text{Al}_{0.53}\text{In}_{0.11}\text{Ga}_{0.36}\text{N}/\text{Al}_{0.58}\text{In}_{0.02}\text{Ga}_{0.40}\text{N}$ MQW. Corresponding data set for the 3.6-nm-thick $\text{Al}_{0.30}\text{Ga}_{0.70}\text{N}/\text{Al}_{0.70}\text{Ga}_{0.30}\text{N}$ MQW are shown in (c) and (d).

since τ_{PL} at 10 K was 2.38 ns for $L=2.9$ nm ($x=0.53$) and 670 ns for $L=3.8$ nm ($x=0.33$).

PL spectrum and energy-resolved τ_{PL} values, and corresponding TRPL signals of the 2.9-nm-thick $\text{Al}_{0.53}\text{In}_{0.11}\text{Ga}_{0.36}\text{N}$ wells are summarized in Figs. 2(a) and 2(b), respectively. Similar data set for the 3.6-nm-thick $\text{Al}_{0.30}\text{Ga}_{0.70}\text{N}$ wells are shown in Figs. 2(c) and 2(d). In Fig. 2(b), normalized PL intensities are vertically shifted for better looking. As shown, the AlInGaN MQW exhibited a *stretched exponential* PL decay shape,¹⁹ as is the case with InGaN and AlInN.^{6,17,20} On the contrary, the curve for the AlGaIn MQW exhibited a biexponential line shape, and τ_{PL} increased with decreasing the photon energy. The results can be explained by the presence of the exponential tail states due to the fluctuations in x , strain, and L ; excitons diffuse from the *free/extended* states to the shallow tail states to recombine. It should be noted that effective τ_{PL} shown in Figs. 2(a) and 2(c) is defined as the time τ after excitation at which $\int_0^\tau I(t)dt / \int_0^{t_{\text{lim}}} I(t)dt$ becomes $1-1/e$, where $I(t)$ is the intensity at time t and t_{lim} is defined for the time at which $I(t_{\text{lim}})$ becomes $0.01I(0)$, in order to compare the recombination processes showing different decay shapes. A remarkable difference between the AlInGaN and AlGaIn MQWs is that the former did not show the spectral diffusion with time but the latter did. The observation of the *stretched exponential* decay without presenting spectral diffusion suggests that excitons in AlInGaN alloys move via hopping process to recombine within the deep localizing centers.¹⁹

Temperature variation of η_{int} and TRPL signal for the 2.9-nm-thick $\text{Al}_{0.53}\text{In}_{0.11}\text{Ga}_{0.36}\text{N}$ wells are shown in Figs. 3(a) and 3(b), respectively. Similar data set for the 3.6-nm-thick $\text{Al}_{0.30}\text{Ga}_{0.70}\text{N}$ wells are shown in Figs. 3(c) and 3(d). Each MQW showed its characteristic decay shape from 10 to 300 K. However, τ_{PL} and η_{int} decreased with the increase in temperature T , especially above 150 K. Values of τ_{PL} for the MQWs are plotted by open triangles in Figs. 4(a) and 4(b), respectively. According to the simplified three-level localized exciton model,¹⁷ the *localization lifetime* τ_{loc} , which represents the combined *transfer and radiative* lifetime of excitons, and nonradiative lifetime in the *free/extended* states ($\tau_{\text{nr,free}}$) of the wells were deduced from the experimental values of τ_{PL} and η_{int} using the relations

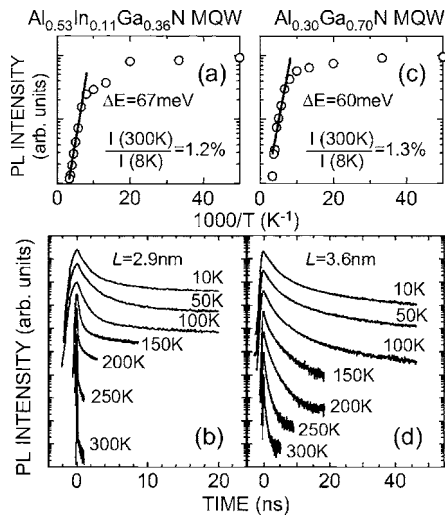


FIG. 3. Temperature variations of (a) η_{int} and (b) TRPL signal for the 2.9-nm-thick $\text{Al}_{0.53}\text{In}_{0.11}\text{Ga}_{0.36}\text{N}/\text{Al}_{0.58}\text{In}_{0.02}\text{Ga}_{0.40}\text{N}$ MQW. Corresponding data set for the 3.6-nm-thick $\text{Al}_{0.30}\text{Ga}_{0.70}\text{N}/\text{Al}_{0.70}\text{Ga}_{0.30}\text{N}$ MQW are shown in (c) and (d).

$1/\tau_{\text{PL}} = 1/\tau_{\text{loc}} + 1/\tau_{\text{nr,free}}$ and $\eta_{\text{int}} = 1/(1 + \tau_{\text{loc}}/\tau_{\text{nr,free}})$, and are plotted by open and closed circles. As shown, critical T , at which $\tau_{\text{nr,free}}$ began to dominate τ_{PL} , for the AlInGaN wells was lower than that for the AlGaN wells, and the $\tau_{\text{nr,free}}$ values at 300 K were 34 ps for the former and 170 ps for the latter. The result indicates that NRC density in the AlInGaN MQW is higher than that in the AlGaN MQW. However, η_{int} at 300 K for the AlInGaN wells (1.2%) was comparable to that for the AlGaN wells (1.3%), meaning that excitons in the AlInGaN alloys are somewhat defect resistant due to the beneficial effect of the exciton localization, as follows. The value of τ_{loc} for the AlGaN MQW was nearly constant below 125 K but increased with T above 150 K (12.9 ns at 300 K), indicating that exciton localization became weaker and thermal escape into *free/extended* states became significant above 150 K. Conversely, τ_{loc} for the $\text{Al}_{0.53}\text{In}_{0.11}\text{Ga}_{0.36}\text{N}$ MQW showed a zero-dimensional behavior, i.e., the value was nearly constant up to 300 K (3.1 ns), indicating that exciton localization is so strong that thermal escape is suppressed. In general, $\text{Al}_x\text{Ga}_{1-x}\text{N}$ alloys of high x exhibit η_{int} lower than 0.1%.^{5,18} Therefore the present result that quaternary wells with $x=0.53$ exhibit $\eta_{\text{int}}=1.2\%$, which is comparable to that for the ternary wells with $x=0.30$, indicates that

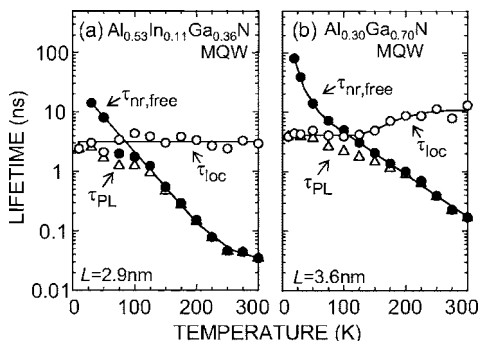


FIG. 4. PL lifetimes τ_{PL} (open triangles) of the (a) 2.9-nm-thick $\text{Al}_{0.53}\text{In}_{0.11}\text{Ga}_{0.36}\text{N}/\text{Al}_{0.58}\text{In}_{0.02}\text{Ga}_{0.40}\text{N}$ and (b) 3.6-nm-thick $\text{Al}_{0.30}\text{Ga}_{0.70}\text{N}/\text{Al}_{0.70}\text{Ga}_{0.30}\text{N}$ MQWs as a function of T . The localization lifetimes τ_{loc} (open circles) and the nonradiative lifetimes in the *free/extended* states $\tau_{\text{nr,free}}$ (closed circles) derived from τ_{PL} and η_{int} are also plotted. Solid lines are drawn to guide the eye.

the doping or alloying with InN is an effective way to improve η_{int} of AlGaN alloys, as is the case with InN into GaN.

In summary, recombination dynamics of the 268 nm PL peak in strained $\text{Al}_{0.53}\text{In}_{0.11}\text{Ga}_{0.36}\text{N}$ wells were shown to be dominated by the exciton localization, since the TRPL signal exhibited a *stretched exponential* decay and the equivalent radiative lifetime was temperature independent. Although the AlN molar fraction in the $\text{Al}_{0.53}\text{In}_{0.11}\text{Ga}_{0.36}\text{N}$ wells was higher and corresponding PL wavelength was shorter than those of the $\text{Al}_{0.30}\text{Ga}_{0.70}\text{N}$ wells, $\eta_{\text{int}}=1.2\%$ was obtained against the presence of $F_{\text{int}} (=1.6 \text{ MV/cm})$ due to the beneficial effect of the exciton localization. The use of $\text{Al}_x\text{In}_y\text{Ga}_{1-x-y}\text{N}$ quaternary alloys was shown to be a hopeful approach to realize deep UV devices.

This work was supported in part by the 21st Century COE program "Promotion of Creative Interdisciplinary Materials Science for Novel Functions" under MEXT, Japan.

- ¹H. Amano and I. Akasaki, *J. Phys.: Condens. Matter* **13**, 9635 (2001); M. Iwaya, S. Terao, T. Sano, S. Takamami, T. Ukai, R. Nakamura, S. Kamiyama, H. Amano, and I. Akasaki, *Phys. Status Solidi A* **188**, 117 (2001).
- ²J. Han, M. H. Crawford, R. J. Shul, J. J. Figiel, M. Banas, L. Zhang, Y. K. Song, H. Zhou, and A. V. Nurmikko, *Appl. Phys. Lett.* **73**, 1688 (1998).
- ³T. Nishida, H. Saito, and N. Kobayashi, *Appl. Phys. Lett.* **78**, 399 (2001).
- ⁴V. Adivarahan, W. H. Sun, A. Chitnis, M. Shatalov, S. Wu, H. P. Maruska, and M. Asif Khan, *Appl. Phys. Lett.* **85**, 2175 (2004).
- ⁵For example, see a review article by H. Hirayama, *J. Appl. Phys.* **97**, 091101 (2005).
- ⁶For example, see S. Nakamura and G. Fasol, *The Blue Laser Diode* (Springer, Berlin, 1997); *Introduction to Nitride Semiconductor Blue Lasers and Light Emitting Diodes*, edited by S. Nakamura and S. F. Chichibu (Taylor & Francis, London, 2000).
- ⁷S. Heikman, S. Keller, S. Newman, Y. Wu, C. Moe, B. Moran, M. Schmidt, U. K. Mishra, J. S. Speck, and S. P. DenBaars, *Jpn. J. Appl. Phys., Part 2* **44**, L405 (2005).
- ⁸F. Bernardini and V. Fiorentini, *Phys. Rev. B* **57**, R9427 (1998).
- ⁹T. Takeuchi, S. Sota, M. Katsuragawa, M. Komori, H. Takeuchi, H. Amano, and I. Akasaki, *Jpn. J. Appl. Phys., Part 1* **36**, L382 (1997).
- ¹⁰S. Chichibu, T. Azuhata, T. Sota, and S. Nakamura, *Appl. Phys. Lett.* **69**, 4188 (1996); S. Chichibu, A. Abare, M. Minsky, S. Keller, S. Fleischer, J. Bowers, E. Hu, U. Mishra, L. Coldren, S. DenBaars, and T. Sota, *ibid.* **73**, 2006 (1998).
- ¹¹P. Lefebvre, S. Anceau, P. Valvin, T. Talierecio, L. Konczewicz, T. Suski, S. P. Lepkowski, H. Teisseyre, H. Hirayama, and Y. Aoyagi, *Phys. Rev. B* **66**, 195330 (2002).
- ¹²S. Nagahama, T. Yanamoto, M. Sano, and T. Mukai, *Jpn. J. Appl. Phys., Part 2* **40**, L788 (2001); S. Masui, Y. Matsuyama, T. Yanamoto, T. Kozaki, S. Nagahama, and T. Mukai, *ibid.* **42**, L1318 (2003).
- ¹³S. Chichibu, K. Wada, and S. Nakamura, *Appl. Phys. Lett.* **71**, 2346 (1997); S. Chichibu, T. Sota, K. Wada, and S. Nakamura, *J. Vac. Sci. Technol. B* **16**, 2204 (1998).
- ¹⁴K. P. O'Donnell, R. W. Martin, and P. G. Middleton, *Phys. Rev. Lett.* **82**, 237 (1999).
- ¹⁵L. Bellaiche, T. Mattila, L.-W. Wang, S.-H. Wei, and A. Zunger, *Appl. Phys. Lett.* **74**, 1842 (1999); P. Kent and A. Zunger, *ibid.* **79**, 1977 (2001).
- ¹⁶S. Keller, P. Waltereit, P. Cantu, U. K. Mishra, J. S. Speck, and S. P. DenBaars, *Opt. Mater. (Amsterdam, Neth.)* **23**, 187 (2003).
- ¹⁷S. F. Chichibu, T. Onuma, T. Aoyama, K. Nakajima, P. Ahmet, T. Chikyow, T. Sota, S. P. DenBaars, S. Nakamura, T. Kitamura, Y. Ishida, and H. Okumura, *J. Vac. Sci. Technol. B* **21**, 1856 (2003); the *localization lifetime* τ_{loc} represents the combined *transfer and radiative* lifetime of the localized states, which increases with temperature T and occupancy of the localized states and decreases with the increase in the localization depth E_{loc} .
- ¹⁸T. Onuma, S. F. Chichibu, A. Uedono, T. Sota, P. Cantu, T. M. Katona, J. F. Keading, S. Keller, U. K. Mishra, S. Nakamura, and S. P. DenBaars, *J. Appl. Phys.* **95**, 2495 (2004).
- ¹⁹R. Kohlrausch, *Ann. Phys.* **12**, 393 (1847).
- ²⁰T. Onuma, S. F. Chichibu, Y. Uchinuma, T. Sota, S. Yamaguchi, S. Kamiyama, H. Amano, and I. Akasaki, *J. Appl. Phys.* **94**, 2449 (2003).